Journal of Advanced Research 35 (2022) 71–86

Contents lists available at ScienceDirect

Journal of Advanced Research

journal homepage: www.elsevier.com/locate/jare

Spred2 controls the severity of Concanavalin A-induced liver damage by limiting interferon-gamma production by CD4$^+$ and CD8$^+$ T cells

Cuiming Sun [a,b], Masayoshi Fujisawa [a], Toshiaki Ohara [a], Qiuying Liu [a], Chen Cao [a], Xu Yang [a], Teizo Yoshimura [a], Steven L. Kunkel [c], Akihiro Matsukawa [a,*]

[a] Department of Pathology and Experimental Medicine, Graduate School of Medicine, Dentistry and Pharmaceutical Sciences, Okayama University, Okayama, Japan
[b] Department of Infectious Disease, The First Hospital of China Medical University, Liaoning, China
[c] Department of Pathology, University of Michigan Medical School, Ann Arbor, MI, USA

HIGHLIGHTS

- Spred2$^{-/-}$ mice developed exacerbated Con A-induced liver damage with increased IFNγ production.
- MEK/ERK inhibitor U0126 markedly inhibited the damage and reduced IFNγ production.
- Neutralization of IFNγ abolished the damage with down-regulated hepatic STAT1 activation.
- Depletion of CD4$^+$/CD8$^+$ T cells improved the damage with decreased IFNγ production.
- Transplantation of CD4$^+$/CD8$^+$ T cells into RAG1$^{-/-}$ mice reproduced severe liver damage.
- Liver damage and IFNγ production were significantly lower in Spred2 transgenic mice.

GRAPHICAL ABSTRACT

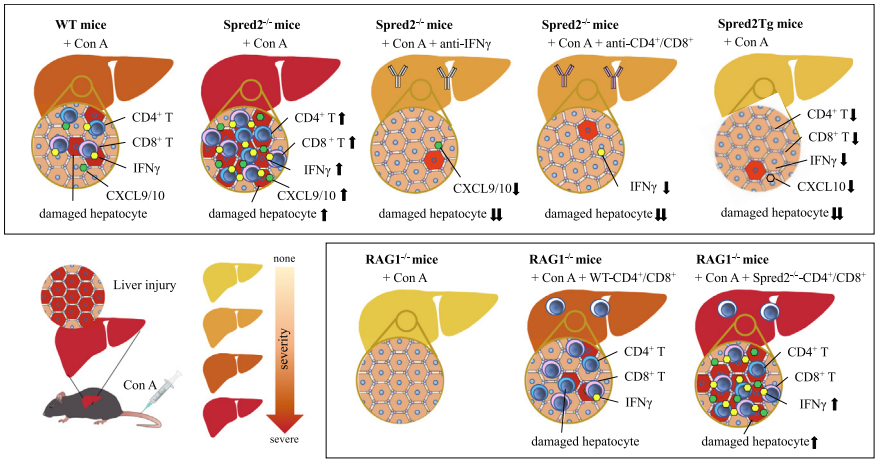

ARTICLE INFO

Article history:
Received 19 October 2020
Revised 12 March 2021
Accepted 30 March 2021
Available online 20 April 2021

Keywords:
Liver damage
MAPK
Signal transduction and regulation
Gene-modified mice
Spred2

ABSTRACT

Introduction: Mitogen-activated protein kinases (MAPKs) are involved in T cell-mediated liver damage. However, the inhibitory mechanism(s) that controls T cell-mediated liver damage remains unknown.
Objectives: We investigated whether Spred2 (Sprouty-related, EVH1 domain-containing protein 2) that negatively regulates ERK-MAPK pathway has a biological impact on T cell-mediated liver damage by using a murine model.
Methods: We induced hepatotoxicity in genetically engineered mice by intravenously injecting Concanavalin A (Con A) and analyzed the mechanisms using serum chemistry, histology, ELISA, qRT-PCR, Western blotting and flow cytometry.
Results: Spred2-deficient mice (Spred2$^{-/-}$) developed more sever liver damage than wild-type (WT) mice with increased interferon-γ (IFNγ) production. Hepatic ERK phosphorylation was enhanced in Spred2$^{-/-}$ mice, and pretreatment of Spred2$^{-/-}$ mice with the MAPK/ERK inhibitor U0126 markedly inhibited the liver damage and reduced IFNγ production. Neutralization of IFNγ abolished the damage with decreased hepatic Stat1 activation in Spred2$^{-/-}$ mice. IFNγ was mainly produced from CD4$^+$ and CD8$^+$ T cells, and their depletion decreased liver damage and IFNγ production. Transplantation of CD4$^+$ and/or CD8$^+$ T cells

Peer review under responsibility of Cairo University.
* Corresponding author.
E-mail address: amatsu@md.okayama-u.ac.jp (A. Matsukawa).

https://doi.org/10.1016/j.jare.2021.03.014

from Spred2$^{-/-}$ mice into RAG1$^{-/-}$ mice deficient in both T and B cells caused more severe liver damage than those from WT mice. Hepatic expression of T cell attractants, CXCL9 and CXCL10, was augmented in Spred2$^{-/-}$ mice as compared to WT mice. Conversely, liver damage, IFNγ production and the recruitment of CD4$^+$ and CD8$^+$ T cells in livers after Con A challenge were lower in Spred2 transgenic mice, and Spred2-overexpressing CD4$^+$ and CD8$^+$ T cells produced lower levels of IFNγ than WT cells upon stimulation with Con A *in vitro*.

Conclusion: We demonstrated, for the first time, that Spred2 functions as an endogenous regulator of T cell IFNγ production and Spred2-mediated inhibition of ERK-MAPK pathway may be an effective remedy for T cell-dependent liver damage.

Introduction

The liver is an immunologic organ prone to viral infection and autoimmune disorders. A major cellular component that causes the hepatic damage is immune cell populations, mainly T cells [1,2]. CD4$^+$ and CD8$^+$ T cells are involved in the development of viral hepatitis and autoimmune hepatitis (AIH) [3,4]. Infiltrating T cells provoke a progressive hepatocyte damage with interface hepatitis, resulting in the progression of liver fibrosis. Understanding a mechanism(s) governing T cell-mediated hepatitis continues to be a significant challenge [1].

When activated, CD4$^+$ and CD8$^+$ T cells generate interferon-γ (IFNγ), and IFNγ production is significantly elevated in patients with viral hepatitis and AIH [5–7]. To elucidate the pathogenesis of T cell-mediated hepatitis, studies using animal models are important. The most frequently used mouse model for investigating T cell-dependent liver damage is a systemic injection of Concanavalin A (Con A) [8]. Con A is an antigen-independent mitogen that activate T cells, resulting in hepatocyte damage [9]. IFNγ directly and indirectly causes hepatocellular apoptosis and necrosis during Con A-hepatotoxicity [10,11]. Con A-hepatotoxicity was ameliorated in mice with IFNγ deficiency [11].

The mitogen-activated protein kinases (MAPKs) are constituted by 3 serine/threonine kinases [12]. Among MAPKs, extracellular regulated kinase (ERK)-1/2 is important in IFNγ responses [13]. ERK activation was found in Con A-induced liver damage and the MAPK/ERK inhibitor U0126 inhibited Con A-stimulated proliferation of CD4$^+$ T cells [14]. Thus, ERK-MAPK overactivation may contribute to exacerbated Con A-hepatotoxicity by enhancing T cell responses, such as IFNγ production.

Signaling pathways are counterbalanced by endogenous inhibitory mechanism(s). Spred2 (Sprouty-related, EVH1 domain-containing protein 2) binds to Ras and inhibits the downstream of the Ras/Raf/ERK-MAPK pathway [15]. We have hitherto investigated the function of Spred2 in several models of acute inflammation and demonstrated that Spred2 in macrophages is essential in downregulating inflammatory responses [16–20]. Spred2-deficient (Spred2$^{-/-}$) mice were vulnerable to hepatotoxicity induced by acetaminophen (APAP) and lipopolysaccharide/D-Galactosamine (LPS/D-Gal) due to up-regulated ERK activation [18,20]. Although the *in vivo* manifestations, represented by increased alanine transaminase (ALT) and tissue damage, are similar among the models, the etiology and molecular mechanism(s) are different. APAP-induced liver injury model represents drug-induced liver injury, in which APAP overdose mainly causes direct hepatocyte injury, resulting in secondary liver damage by subsequent leukocyte responses [21]. LPS/D-Gal-induced liver injury model represents liver injury during sepsis, which is suitable for investigating TNFα-mediated apoptosis [22]. Con A-hepatotoxicity is a model of T cell-mediated liver damage [8], which is regarded as a relevant model of viral hepatitis and AIH. To gain a deeper understanding of the function(s) of Spred2 in liver pathology, it is vitally important to explore the molecular mechanisms in all these liver injury models.

In the present study, we aimed to investigate whether Spred2 plays any role in T cell-mediated liver damage by injecting Con A into Spred2$^{-/-}$ and Spred2 transgenic (Spred2Tg) mice. We demonstrated that endogenous Spred2 is protective in Con A-hepatotoxicity by inhibiting CD4$^+$ and CD8$^+$ T cell IFNγ production via downregulating the ERK-MAPK pathway.

Materials and methods

Reagents

Con A was obtained from Sigma-Aldrich (St. Louis, MO, USA). Recombinant mouse IFNγ and U0126 were purchased from BioLegend (San Diego, CA, USA) and Promega (Madison, WI, USA), respectively. Antibodies used for Western blotting and flow cytometry were listed in Table 1.

Mice

The generation of Spred2$^{-/-}$ mice in C57BL/6J background were previously described [23]. C57BL/6J mice were employed as wild-type mice (WT). RAG1 (recombination-activating protein 1) deficient mice (RAG1$^{-/-}$) were obtained from Charles River Laboratories (Yokohama, Japan). To generate Spred2-overexpresion mice (Spred2Tg), *pCAGGS-Spred2* expression vector was constructed by inserting coding region of *Spred2* cDNA into a pCAGGS vector, which contains CAG promoter (chimeric promoter of CMV IE

Table 1
Antibodies for Western blotting and flow cytometry.

Western blotting	
Bcl2	Cell Signaling Technology (3498)
GAPDH	Cell Signaling Technology (5174)
p44/42 MAPK (ERK1/2)	Cell Signaling Technology (4695)
phospho-p44/42 MAPK (pERK1/2) (Thr 202/Tyr 204)	Cell Signaling Technology (4370)
STAT1	Cell Signaling Technology (9172)
phospho-STAT1 (Tyr 701)	Cell Signaling Technology (9167)
STAT3	Cell Signaling Technology (12640)
phospho-STAT3 (Tyr 705)	Cell Signaling Technology (9145)
HRP-goat anti-rabbit IgG	Cell Signaling Technology (7074)
HRP-anti-mouse IgG	Cell Signaling Technology (7076)
Flowcytometry	
CD16/32	BioLegend (101302)
FITC-CD3 (17A2)	BioLegend (100204)
PE-CD4 (GK1.5)	BD Pharmingen (553730)
FITC-CD8 (53–6.7)	BioLegend (100706)
PE-CD8 (53–6.7)	BioLegend (100708)
PE-NK1.1 (PK136)	BioLegend (108708)
FITC-IFNγ (XMG1.2)	BioLegend (505806)

enhancer and chicken beta-actin promoter), chicken beta-actin 1st intron, rabbit beta-globin second intron, third exon and 3′ flanking region [24](Fig. S1). Coding region sequence of *Spred2* cDNA was chemically synthesized with the Kozak consensus sequence at 5′ end and *Eco*RI site at both ends. Synthesized fragment was digested with *Eco*RI and inserted at *Eco*RI site on pCAGGS vector, between beta-globin third intron and 3′ flanking region (Fig. S1). The purified transgene DNA was used for micro-injection into the pronucleus of C57BL/6 mouse fertilized eggs, and eggs were transferred to the oviducts of pseudo-pregnant mice to generate transgenic mice. For genotyping of transgenic mice, following primer set was used; pCAGGS-F1: 5′-GTCGACATTGATTATTGACTAGTTATTAA TATGAATC-3′ and R2275: 5′-GTCGAGGGATCTCCATAAGAGAA GAGGCAGA-3′. Eighty-two mice were obtained from injected embryos, and 7 mice had the transgene. The founder mice were then crossed with C57BL/6J wild-type females, and hemizygous F1 mice were obtained. Generation of transgenic mice was performed in Transgenic Inc. (Kobe Japan) with institutional Animal Research Committee approval. Hemizygous mice were then crossed with C57BL/6J mice, and mice with transgene were used as Spred2Tg mice. Non-transgenic littermates were used as WT mice.

All mice used in this study were bred and maintained under a continuous 12 h light/12 h dark cycle in a specific pathogen-free condition at the Department of Animal Resources, Okayama University (Okayama, Japan). Female mice (6–8 weeks of age) were employed in this study.

Ethics statement

All experiments involving animals were conducted according to the ethical policies and procedures approved by The Animal Care and Use Committee of Okayama University (Approved No. OKU-2016557, OKU-2019034).

Liver injury model

Con A (10 mg/kg body weight) was injected once into mice through tail vein to induce acute liver damage. At indicated times after Con A challenge, mice were anesthetized and euthanized. After perfusion with sterile saline, livers were resected and stored at −80 °C for detection of mRNA and protein expression. Part of the liver was fixed with 10% formalin solution and 4-μm paraffin sections were stained with hematoxylin and eosin (HE). Three independent pathologists evaluated the sections. To measure %injured area, HE sections were captured under microscope and analyzed using a microscopy imaging software (cellSens Standard; Olympus, Tokyo, Japan). For monitoring mice survival, mice were received a sublethal dose (15 mg/kg) of Con A through tail vein. In different sets of experiments, mice were intraperitoneal administered with 10 μmol/kg U0126 or vehicle (DMSO) 3 h prior to 10 mg/kg Con A injection. To neutralize endogenous IFNγ, rabbit anti-mouse IFNγ IgG or control rabbit IgG (1 mg/mouse) was intraperitoneally injected 12 h prior to 10 mg/kg Con A. To deplete $CD4^+$ or $CD8^+$ T cells, mice received intraperitoneal administration of anti-CD4 (L3T4, 100 μg/mouse) or anti-CD8 mAb (Lyt-2.2, 100 μg/mouse) [25], 12 h prior to 10 mg/kg Con A. Isotype matched control rat IgG was used as control.

Caspase assay

Livers were homogenized, centrifuged, and the cleared supernatants were harvested. One hundred μg of extracts were used for measuring caspase-3, caspase-8, and caspase-9 activities (Colorimetric assay kits; MBL, Nagoya, Japan).

Cell isolation and culture

Splenocytes were harvested from spleens after dispersing into cell-suspensions. $CD4^+$ and $CD8^+$ T cells were isolated from splenocyte-suspensions (purity and %alive cells > 95%) using $CD4^+$ and $CD8a^+$ T cell isolation kit (Miltenyi Biotec, Bergisch Gladbach, Germany), respectively. Cells (5×10^6 cells/mL) were cultured with 10 μg/mL Con A.

Leukocyte isolation from livers

After perfusion with saline, livers were removed, chopped and digested with 5 mL digestion buffer (HBSS containing 20 mM HEPES, pH 7.4, plus 0.02% w/v collagenase, 0.0005% w/v DNase I) for 30 min using gentleMACS™ Dissociator (Miltenyi Biotec). After filtering through 100-μm nylon mesh, cells were washed, centrifuged, and the resultant cell pellets were suspended in 35% Percoll. After centrifugation, cell pellets were washed, and cell numbers were counted under microscope.

Hepatocyte isolation and culture

Hepatocyte isolation was carried out, as described previously [26]. Isolated hepatocytes (>95% alive) were suspended in hepatocyte maintenance medium (Thermo fisher), distributed onto collagen I-coated plates (1.3×10^5 cells/well, CORNING, Kennebunk, ME, USA) and incubated overnight. Hepatocytes were cultured with 40 ng/mL IFNγ for 6 h (for chemokine expression by cells) or 48 h (for lactate dehydrogenase (LDH) release in the supernatants).

Cell transplantation

Purified $CD4^+$ T cells (2.5×10^6 cells/mouse) or $CD8^+$ T cells (5×10^6 cells/mouse) were injected into $RAG1^{-/-}$ mice deficient in both T and B cells through tail vein, 1 week before 10 mg/kg Con A challenge.

Real-time quantitative PCR (RT-qPCR)

Total RNA was isolated from cells and livers using High Pure RNA Isolation Kit (Roche Applied Science, Mannheim, Germany) and Trizol Reagent (Thermo Fisher), respectively. First-strand cDNAs were synthesized from 2 μg total RNA using High capacity cDNA reverse transcription kit (Thermo Fisher). RT-qPCR was run on a StepOnePlus system (Thermo Fisher). Gene expression level of interest was normalized using that of GAPDH expression. Taqman gene expression assays (Thermo Fisher) used in this study were shown in Table 2.

Western blotting

Cells and livers were lysed in a lysis buffer (Cell Signaling), centrifuged, and cleared supernatants were harvested. Proteins in each lysate (10 μg) were fractionated by SDS-polyacrylamide gel electrophoresis (Thermo Fisher) and transferred onto nitrocellulose membranes. After blocking, the membranes were incubated overnight with a primary antibody. The membranes were washed and then incubated with horseradish peroxidase-conjugated secondary antibody. Target proteins were visualized by ImmunoStar LD (Wako, Osaka, Japan) and quantitated using C-DiGit Blot scanner (LI-COR Biotechnology, Lincoln, Nebraska, USA). The images were semi-quantitated with Image Studio software.

Table 2
Taqman gene expression assays used for RT-qPCR.

Gene	Taqman gene expression assay kit
IFNγ	Mm 01168134_m1
TNFα	Mm00443258_m1
IL-12p40	Mm00434174_m1
CXCL9	Mm 00434946_m1
CXCL10	Mm 00445235_m1
granzyme B	Mm00442834_m1
perforin	Mm00812512_m1
Spred2	Mm01223872_g1
GAPDH	Mm 99999915_g1

Flow cytometry

After Fc blocking with anti-CD16/CD32 antibody, cells were incubated with antibodies of interest or isotype control rat IgG and cell populations were examined using a Cell Lab Quanta SC MPL (Beckman Coulter, Inc., Brea, CA). Lymphocytes were gated using Electronic Volume (EV) versus Side Scatter (SS) in a dual parameter gate, and then analyzed the percentage of each cell population among gated lymphocytes. For IFNγ intracellular staining, IFNγ antibody was diluted in fixation/permeabilization buffers (eBioscience, San Diego, CA, USA). The number of each leukocyte population per liver was determined from the respective percentage and total number of hepatic leukocytes.

Elisa

IFNγ, TNFα and IL-12 levels were determined using a standard sandwich ELISA (BioLegend). These ELISAs did not recognize other murine cytokines available.

Statistics

Data were analyzed using GraphPad Prism 7 (GraphPad Software, San Diego, CA, USA). After assessments of the normality of data, statistical significance was analyzed by parametric two-tailed unpaired *t* test and non-parametric Mann Whitney *u* test for normal distribution and non-normal distribution, respectively. Data were expressed as the mean ± SEM, (normal distribution) or median ± range (non-normal distribution). All test results including mean, median, range, exact-*p* value and test method were summarized in supplementary table 1. Survival rate was compared using the log-rank test. A p value < 0.05 was considered statistically significant.

Results

Spred2$^{-/-}$ mice exhibit exacerbated liver damage via enhanced ERK activation

To examine a potential involvement of Spred2 in Con A-hepatotoxicity, we employed Spred2$^{-/-}$ mice. No difference was found in serum ALT level between naive WT and Spred2$^{-/-}$ mice (65.0 ± 5.0 vs 53.3 ± 14.5 IU/L, respectively, 4 mice each). Upon injection of 10 mg/kg Con A, increased ALT levels (Fig. 1A) and augmented injured area represented by hepatocyte necrosis with infiltrating leukocytes (Fig. 1B) were detected in Spred2$^{-/-}$ mice relative to WT mice. Survival rate of Spred2$^{-/-}$ mice after injecting a sublethal dose (15 mg/kg) of Con A was lower than that of WT mice (Fig. 1C). Con A-hepatotoxicity is shown to be accompanied by increased caspases activates, important for the induction of hepatocyte apoptosis [27]. As shown in Fig. 1D, activities of caspase-3, −8, and −9 in Spred2$^{-/-}$-livers after 10 mg/kg Con A challenge were significantly augmented, as compared to WT-livers. In contrast, hepatic levels of bcl-2, anti-apoptotic factor, were reduced in Spred2$^{-/-}$-livers as compared to WT-livers (Fig. 1E). Thus, Spred2-deficiency is deleterious in Con A-induced liver damage.

The key molecules involved in Con A-hepatotoxicity are MAPKs, including ERK [14]. The enhanced hepatotoxicity in Spred2$^{-/-}$ mice may result from the augmented ERK-MAPK pathway. As shown in Fig. 1F, activation of ERK, indicated by phosphorylated ERK/total ERK (pERK/tERK) ratio, was weak in livers from untreated WT and Spred2$^{-/-}$ mice. ERK activation at 12 h post Con A challenge was evident in WT-livers, which was further augmented in Spred2$^{-/-}$-livers (Fig. 1F). U0126, a MAPK/ERK inhibitor, reduced ERK activation in WT- and Spred2$^{-/-}$-livers (Fig. 1G), and protected WT and Spred2$^{-/-}$ mice from liver damage, as estimated by decreased ALT levels (Fig. 1H) and reduced injured area (Fig. 1I). These data indicated that exacerbated liver damage in Spred2$^{-/-}$ mice was dependent on enhanced ERK activation.

IFNγ is ascribed to enhanced hepatotoxicity in Spred2$^{-/-}$ mice

Since T helper 1 cytokines that include IFNγ, TNFα and IL-12 are known involved in Con A-hepatotoxicity [28], levels of these cytokines were examined. At 12 h post Con A challenge, hepatic IFNγ mRNA expression level and serum IFNγ level in Spred2$^{-/-}$ mice were higher than that in WT mice (Fig. 2A, B). No differences were found in the expression of TNFα and IL-12 at mRNA and protein level between WT and Spred2$^{-/-}$ mice (Fig. 2A, B). Increased IFNγ levels in livers (Fig. 2C) and circulation (Fig. 2D) were reduced by U0126, both in WT and Spred2$^{-/-}$ mice, relative to control.

In response to Con A, Stat proteins, such as Stat1 and Stat3, are activated and mediate liver damage [29]. Fig. 3A demonstrated that phosphorylation of Stat1, but not Stat3, was increased in Spred2$^{-/-}$-livers as compared to WT-livers after Con A challenge. STAT1 in the liver is predominately activated by IFNγ, and we found neutralization of IFNγ in Spred2$^{-/-}$ mice decreased Stat1 activation, but not Stat3 activation, in the liver (Fig. 3B). Interestingly, U0126 treatment of Spred2$^{-/-}$ mice significantly decreased Stat1 activation in Spred2$^{-/-}$-livers relative to the controls (Fig. 3C). To further elucidate the contribution of IFNγ to the liver damage in Spred2$^{-/-}$ mice, the degree of liver damage was evaluated after neutralization of IFNγ. Neutralization of IFNγ dramatically reduced Con A-hepatotoxicity in Spred2$^{-/-}$ mice, as serum levels of ALT were inhibited by 93% (Fig. 3D) and injured area were reduced by 94% by histological examination (Fig. 3E), as compared to controls. These results indicate that exacerbated hepatotoxicity in Spred2$^{-/-}$ mice is ascribed to the enhanced IFNγ production. Further, the enhanced IFNγ production in Spred2$^{-/-}$ mice was due to the enhanced ERK-MAPK signaling, potentially in T cells, resulting in subsequent Stat1 activation and exacerbated liver damage.

CD4^{+} and CD8^{+} T cells are ascribed to increased IFNγ production and liver damage in Spred2$^{-/-}$ mice

We examined the effect of Spred2-deficiency on the capacity of T cells to produce IFNγ. We first isolated splenocytes from Con A-treated mice and cultured for 24 h without additional stimulation. As shown in Fig. 4A, Spred2$^{-/-}$-splenocytes released higher level of IFNγ than WT controls. Next, splenocytes from naive mice were stimulated with Con A *in vitro*. Again, Spred2$^{-/-}$-splenocytes produced higher levels of IFNγ than WT controls (Fig. 4B). ERK activation is important for T cell function [30]. As shown in Fig. 4C, ERK activation in naive WT- and Spred2$^{-/-}$-splenocytes was weak, which was significantly augmented in Spred2$^{-/-}$-splenocytes after Con A stimulation as compared to WT controls. IFNγ activates Stat1 signaling pathway during Con A-hepatotoxicity [29]. Stat1 is known activated in CD4^{+} T cells after Con A injection *in vivo* [31,32]. As shown in Fig. 4D, Stat1 activation in Spred2$^{-/-}$-

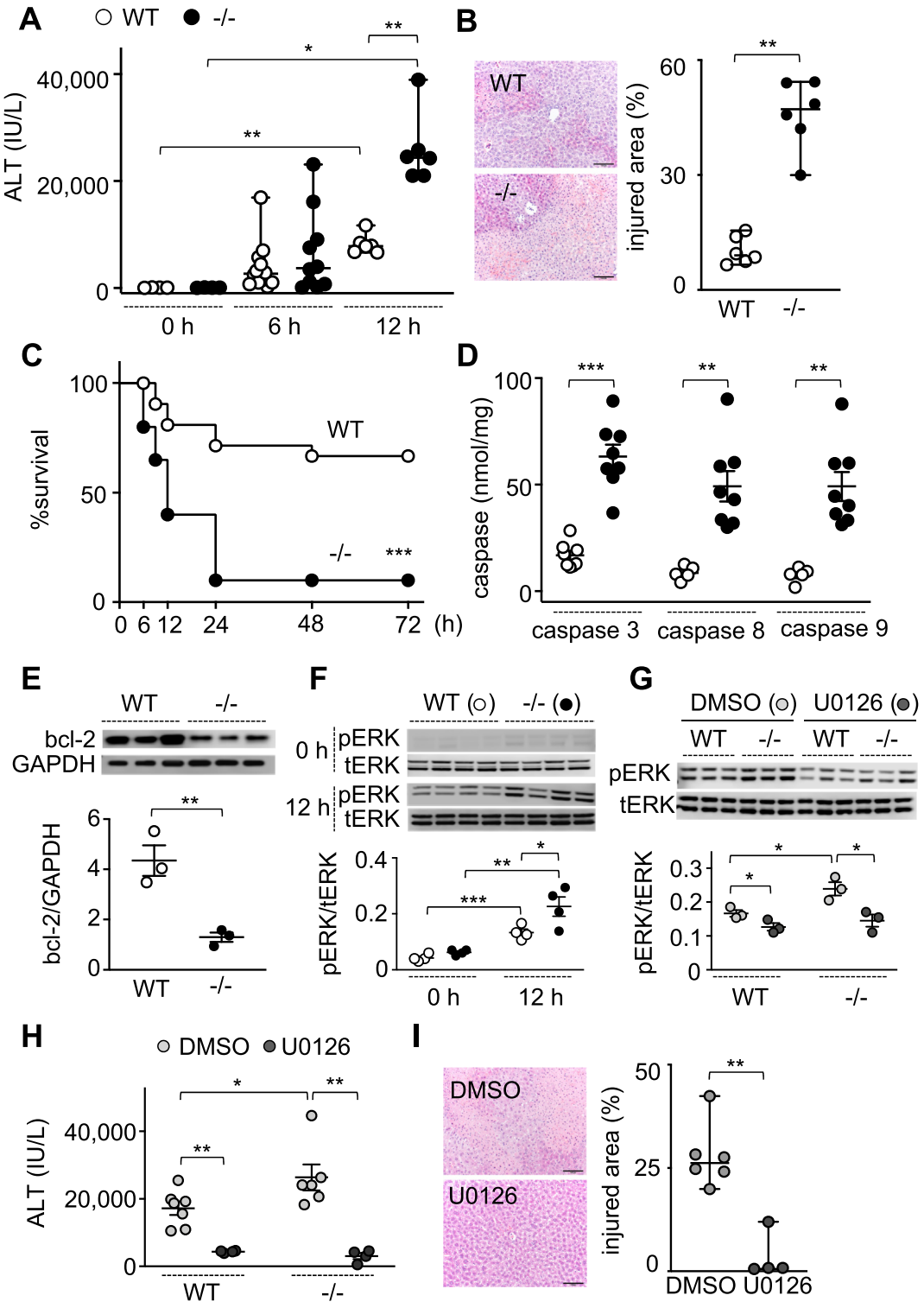

Fig. 1. Spred2$^{-/-}$ mice exhibit exacerbated Con A-induced liver damage via enhanced ERK activation. (A) Serum ALT levels in WT and Spred2$^{-/-}$ mice were measured post 10 mg/kg Con A challenge (4–12 mice, each). (B) Left; liver sections from WT and Spred2$^{-/-}$ mice at 12 h post 10 mg/kg Con A challenge (scale bar, 100 μm). Right; %injured area was estimated using cellSens Standard software (6 mice, each). (C) Survival of WT (20 mice) and Spred2$^{-/-}$ mice (20 mice) after a sublethal dose (15 mg/kg) of Con A challenge was monitored. (D) Caspase-3, −8, −9 activities in WT-livers (5–8 mice) and Spred2$^{-/-}$-livers (8 mice) were determined at 12 h post 10 mg/kg Con A challenge. (E,F) Liver extracts at 12 h post 10 mg/kg Con A challenge were immunoblotted with indicated primary antibodies (E; 3 mice each, F; 4 mice each). Band densities were digitised and semi-quantitated. (G,H) WT and Spred2$^{-/-}$ mice were intraperitoneally injected with 10 μmol/kg U0126 or DMSO 3 h before 10 mg/kg Con A challenge. (G) The level of each protein in livers at 12 h post 10 mg/kg Con A challenge was evaluated by Western blotting using the indicated primary antibodies (3 mice each). Band densities were semi-quantitated. (H) ALT levels in the sera at 12 h post 10 mg/kg Con A challenge were measured (DMSO; 6 mice, U0126; 4 mice). (I) Spred2$^{-/-}$ mice were intraperitoneally injected with 10 μmol/kg U0126 or DMSO 3 h before 10 mg/kg Con A challenge. Left; representative photographs of liver sections at 12 h post Con A challenge (scale bar, 100 μm). Right; %injured area was estimated using cellSens Standard software (DMSO; 6 mice, U0126; 4 mice). *p < 0.05., **p < 0.01., ***p < 0.001.

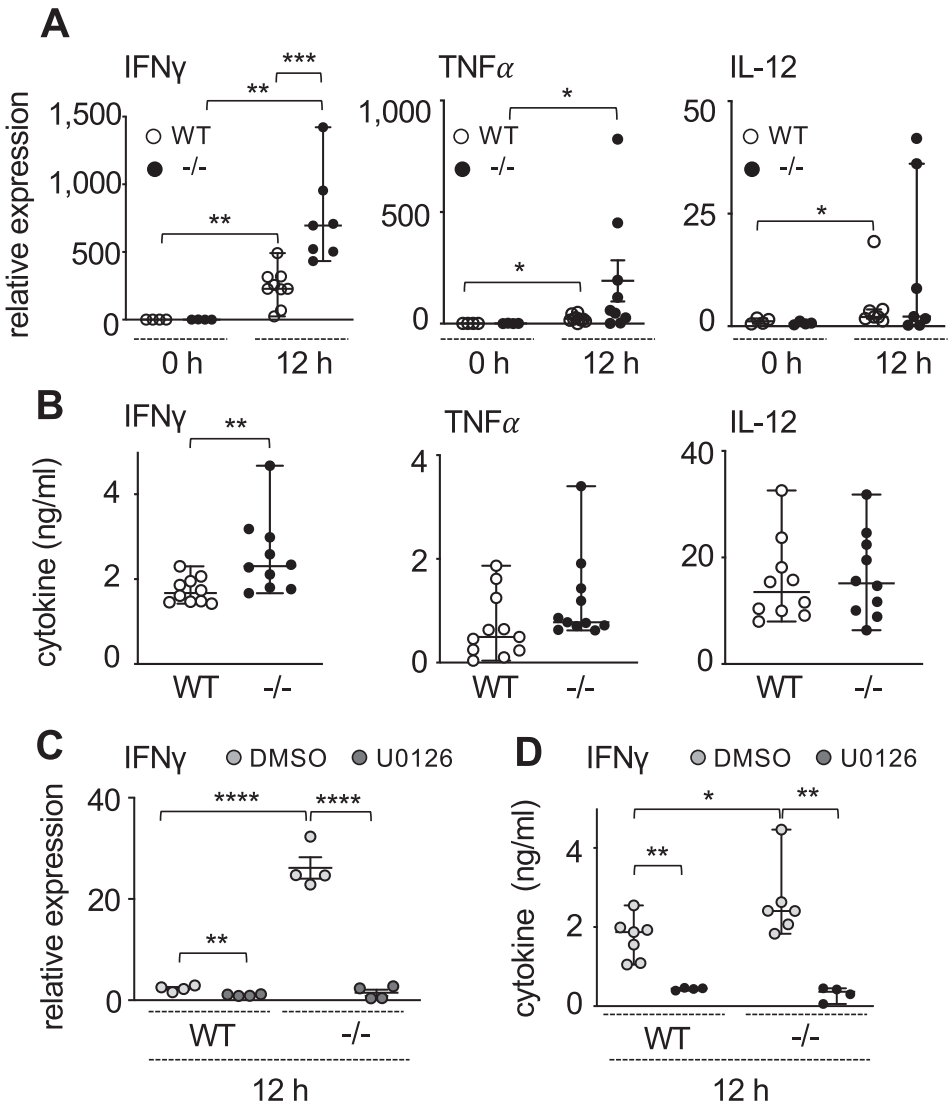

Fig. 2. Cytokine response in Spred2$^{-/-}$ mice. (A) IFNγ, TNFα and IL-12 p40 mRNA expressions in WT- and Spred2$^{-/-}$-livers after 10 mg/kg Con A challenge were analyzed by RT-qPCR (4–10 mice, each time point). (B) Serum IFNγ, TNFα and IL-12 levels in WT and Spred2$^{-/-}$ mice at 12 h post 10 mg/kg Con A challenge were measured by ELISA (10–11 mice, each). (C,D) WT and Spred2$^{-/-}$ mice were intraperitoneally administered with 10 μmol/kg U0126 or DMSO 3 h prior to 10 mg/kg Con A challenge. IFNγ mRNA expression in livers (C) and IFNγ level in sera (D) at 12 h post Con A challenge were evaluated by RT-qPCR and ELISA, respectively (4–6 mice, each). *$p < 0.05$., ** $p < 0.01$., ***$p < 0.001$., **** $p < 0.0001$.

splenocytes was significantly higher, compared to WT-controls. U0126 dramatically abolished the Stat1 activation in both WT- and Spred2$^{-/-}$-splenocytes (Fig. 4E). Thus, splenocytes produce IFNγ in response to Con A, which was enhanced in Spred2$^{-/-}$-cells through augmented ERK activation, resulting in subsequent Stat1 activation.

We next investigated T cell infiltration in livers after Con A challenge. The total number of leukocytes at 12 h post Con A challenge was increased in Spred2$^{-/-}$-livers compared to WT-livers (Fig. 5A). Flow cytometry showed that the percentage and the number of infiltrating CD4$^+$ and CD8$^+$ T cells were higher in Spred2$^{-/-}$-livers than in WT-livers (Fig. 5B). No differences were found in the percentage and the number of NKT and NK cells between the groups. Numbers of CD4$^+$ T, CD8$^+$ T, NKT, and NK cells were similar between naive WT and Spred2$^{-/-}$ mice (0.73 ± 0.08 vs 0.94 ± 0.08 × 10^6 cells, 0.19 ± 0.05 vs 0.18 ± 0.03 × 10^6 cells, 0.33 ± 0.09 vs 0.57 ± 0.05 × 10^6 cells, 0.72 ± 0.11 vs 0.75 ± 0.06 × 10^6 cells respectively, 4 mice each). To examine the cellular source of enhanced IFNγ production in livers, we performed intracellular IFNγ staining. Fig. 5C demonstrated that numbers of IFNγ-producing CD4$^+$ and CD8$^+$ T cells in Spred2$^{-/-}$-livers were higher than WT-livers, while those of NKT and NK cells were comparable between the groups. To further confirm the results, splenic CD4$^+$ and CD8$^+$ T cells from naive WT and Spred2$^{-/-}$ mice were stimulated with Con A *in vitro*. Both WT-CD4$^+$/CD8$^+$ T cells constitutively expressed Spred2, and expression levels were increased at 6 h after Con A stimulation (Fig. S2), suggesting a role of endogenous Spred2 in T cell function. Upon stimulation with Con A, Spred2$^{-/-}$-CD4$^+$ and CD8$^+$ T cells generated higher levels of IFNγ than WT controls (Fig. 5D) .To verify the enhanced IFNγ producing capability of CD4$^+$ and CD8$^+$ T cells in Spred2-deficiency, Spred2$^{-/-}$-CD4$^+$ and CD8$^+$ T cells were cultured with anti-CD3/CD28, which provides antigen-independent signaling of the TCR complex [33]. Under the conditions, enhanced IFNγ production in Spred2$^{-/-}$-CD4$^+$ and -CD8$^+$ T cells were also observed (Fig. 5E). When ERK pathway was blocked by U0126, higher production of IFNγ in Spred2$^{-/-}$-CD4$^+$ and -CD8$^+$ T cells were

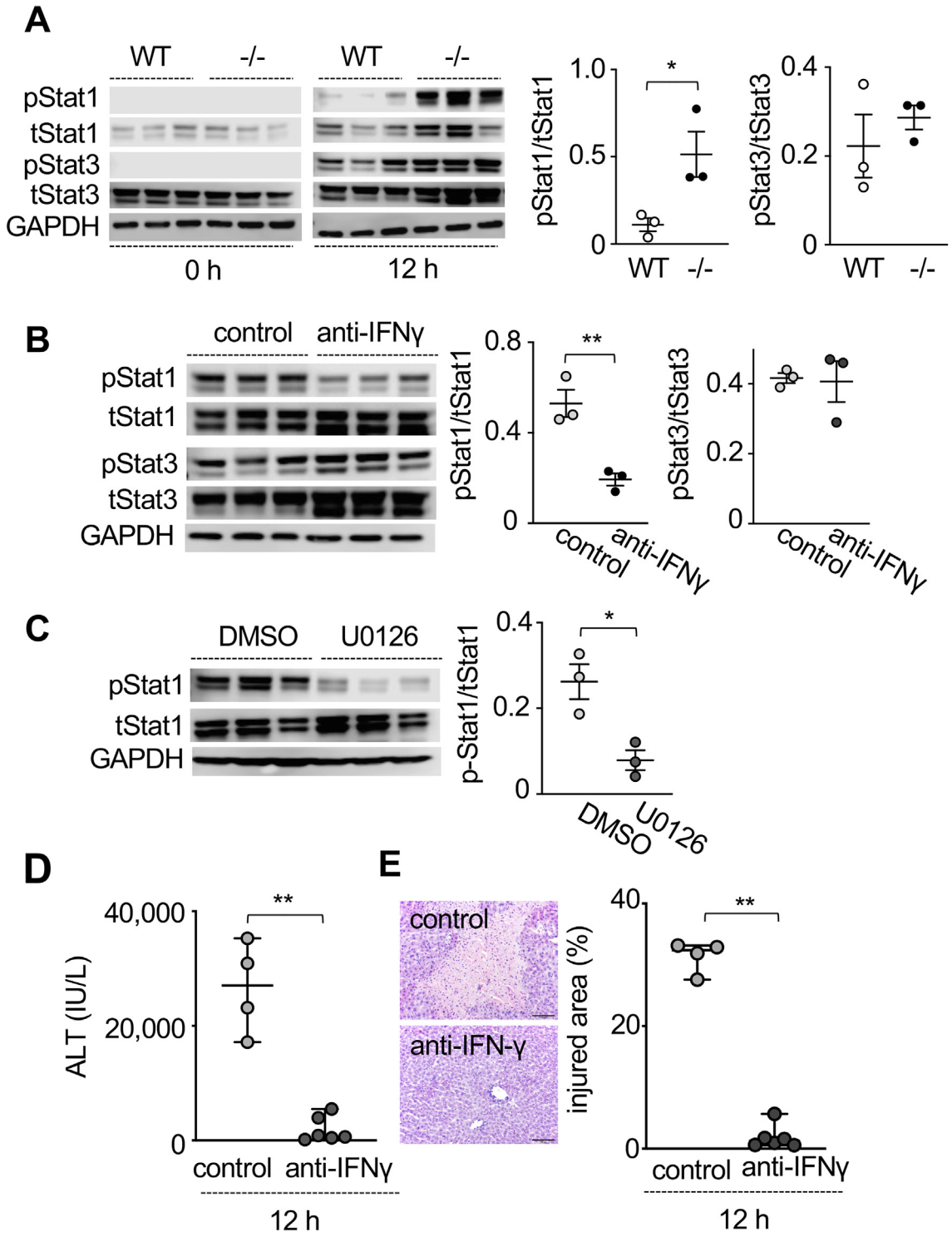

Fig. 3. Neutralization of IFNγ reduces Con A-induced Stat1 activation and liver damage. (A) Con A (10 mg/kg) was intravenously injected into WT and Spred2$^{-/-}$ mice. The level of each protein in liver extracts at 12 h post Con A challenge was evaluated by Western blotting using the indicated primary antibodies (3 mice, each). Band densities were semi-quantitated at 12 h post Con A challenge. (B) Spred2$^{-/-}$ mice were intraperitoneally administered with anti-mouse IFNγ IgG (1 mg/mouse) or control rabbit IgG 12 h prior to 10 mg/kg Con A challenge. The level of each protein in liver extracts at 12 h post Con A challenge was evaluated by Western blotting using the indicated primary antibodies (3 mice, each). Band densities were semi-quantitated. (C) Spred2$^{-/-}$ mice were intraperitoneal injected with 10 μmol/kg U0126 or DMSO 3 h prior to 10 mg/kg Con A challenge. The level of each protein in liver extracts at 12 h post Con A challenge was evaluated by Western blotting using the indicated primary antibodies (3 mice per group). Band densities were semi-quantitated. (D, E) Anti-mouse IFNγ IgG (1 mg/mouse) or control rabbit IgG was intraperitoneally injected into Spred2$^{-/-}$ mice 12 h prior to 10 mg/kg Con A challenge. (D) Serum ALT levels at 12 h post Con A challenge were measured (control; 4 mice, anti-IFNγ-treated; 6 mice). (E) Left; representative photographs of H&E-stained liver sections (scale bar, 100 μm) are shown. Right; %injured area was estimated using the cellSens Standard software (control; 4 mice, anti-IFNγ-treated; 6 mice). $^{*}p < 0.05$., $^{**}p < 0.01$.

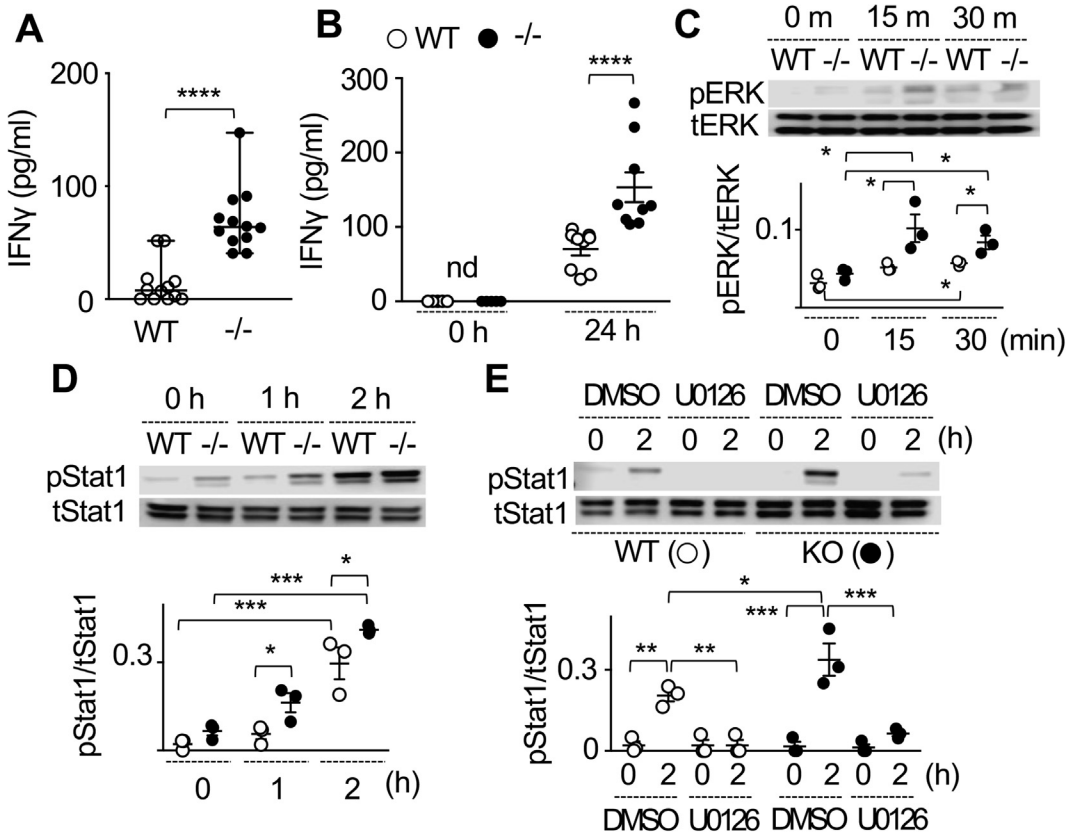

Fig. 4. Enhanced IFNγ production in Spred2-deficiency with augmented activation of ERK and Stat1. (A) Splenocytes harvested from WT and Spred2$^{-/-}$ mice at 12 h post 10 mg/kg Con A challenge were cultured for 24 h without additional stimulation (n = 12). IFNγ levels in the culture supernatants were measured. (B) Splenocytes harvested from naive WT and Spred2$^{-/-}$ mice were cultured with 10 μg/mL Con A for 24 h (n = 9). IFNγ levels in the culture supernatants were quantitated. (C) Splenocytes isolated from naive WT and Spred2$^{-/-}$ mice were cultured with 10 μg/mL Con A for 15 and 30 min. The level of each protein in cells was evaluated by Western blotting using the indicated primary antibodies (3 each). Band densities were semi-quantitated. (D, E) Splenocytes isolated from naive WT and Spred2$^{-/-}$ mice were cultured with 10 μg/mL Con A (D) and 10 μM U0126 or DMSO (E) for 1 and 2 h. The level of each protein in cells was evaluated by Western blotting using the indicated primary antibodies (3 each). Band densities were digitised and semi-quantitated. *p < 0.05., **p < 0.01., ***p < 0.001., **** p < 0.0001.

dramatically reduced after either Con A (Fig. 5F) or anti-CD3/CD28 stimulation (Fig. 5G). Thus, Spred2-deficiency results in a higher T cell IFNγ producing capacity.

CD4$^+$ and CD8$^+$ T cells are attracted by IFNγ-inducible chemokine CXCL9 and CXCL10 [34]. In Spred2$^{-/-}$ mice, hepatic mRNA levels of CXCL9 and CXCL10 at 12 h post Con A challenge were higher than WT controls, while CXCL9 level was not statistically significant between the groups (Fig. 6A). Hepatic mRNA expression of CXCL9 and CXCL10 in Spred2$^{-/-}$ mice was reduced by 79% and 97%, respectively, after IFNγ neutralization (Fig. 6B), indicating that IFNγ induced CXCL9 and CXCL10 mRNA expression in Spred2$^{-/-}$ mice. U0126 treatment reduced not only IFNγ (Fig. 2C,D) but CXCL9 and CXCL10 expressions in both WT- and Spred2$^{-/-}$-livers (Fig. 6C). IFNγ was previously shown to stimulate hepatocytes to produce CXCL9 and CXCL10 [35,36]. Upon IFNγ stimulation for 6 h *in vitro*, primary hepatocytes (purity > 95%) harvested from naive Spred2$^{-/-}$ mice expressed increased CXCL9 and CXCL10 levels compared with WT controls (Fig. 6D). Thus, increased IFNγ production in Spred2$^{-/-}$ mice induced enhanced CXCL9 and CXCL10 expression, possibly leading to augmented infiltration of CD4$^+$ and CD8$^+$ T cells in livers.

CD4$^+$ and CD8$^+$ T cells are responsible for enhanced hepatotoxicity in Spred2$^{-/-}$ mice

To further define the biological function of CD4$^+$ and CD8$^+$ T cells in enhanced Con A-hepatotoxicity in Spred2$^{-/-}$ mice, Spred2$^{-/-}$ mice were intraperitoneally injected with anti-CD4$^+$, anti-CD8$^+$ antibody, or control rat IgG 12 h prior to Con A challenge (Fig. S3). In Spred2$^{-/-}$ mice, depletion of CD4$^+$ and CD8$^+$ T cells reduced ALT level by 95.7% and 46.1%, respectively. No additional reduction was found after injection of both anti-CD4$^+$ and anti-CD8$^+$ antibody (Fig. 7A). Serum levels of IFNγ (Fig. 7B) and IFNγ expressions in livers (Fig. 7C) were significantly decreased after depletion of CD4$^+$ and CD8$^+$ T cells. Next, CD4$^+$ and CD8$^+$ T cells isolated from naive WT and Spred2$^{-/-}$ mice were transplanted into RAG1$^{-/-}$ mice deficient in both T and B cells (Fig. S4). Consistent with previous studies [37], no increase in ALT level was found in RAG1$^{-/-}$ mice at 12 h post Con A challenge (non-treated; 29.5 ± 1. 3 IU/L., 12 h post ConA challenge; 25.3 ± 3.4 IU/L, 4 mice each). RAG1$^{-/-}$ mice received Spred2$^{-/-}$-CD4$^+$ and CD8$^+$ T cells showed enhanced liver damage after Con A challenge, as estimated by increased levels of serum ALT (Fig. 7D,G) and histological tissue damage (Fig. 7E,H), relative to those transferred with WT-cells. Serum IFNγ levels were also increased in mice transferred with Spred2$^{-/-}$-CD4$^+$ and CD8$^+$ T cells (Fig. 7F,I). Interestingly, Con A-induced tissue damage upon Spred2$^{-/-}$-CD4$^+$ T cell transfer was more severe than Spred2$^{-/-}$-CD8$^+$ T cell transfer, despite the number of transferred CD8$^+$ T cells was twice as many as that of CD4$^+$ T cells. Together with the neutralizing studies (Fig. 7A,B), Spred2-deficiency in CD4$^+$ T cells may be more critical in liver damage than that in CD8$^+$ T cells in Con A-hepatotoxicity.

CD8$^+$ T cells may exhibit the cytolytic activity by releasing perforin and granzyme B [38]. Although no differences were found in perforin and granzyme B mRNA expressions between

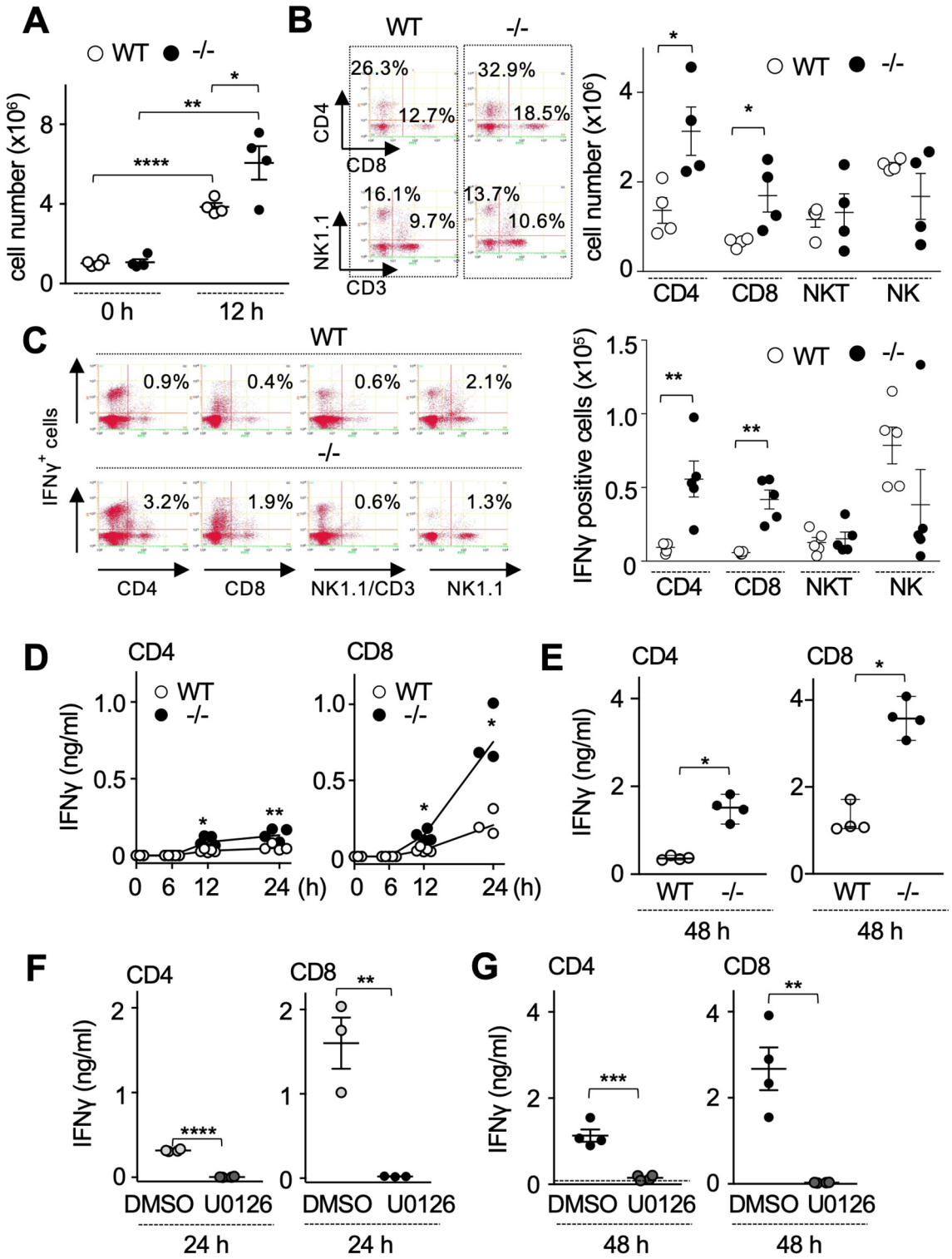

Fig. 5. $CD4^+$ and $CD8^+$ T cells are responsible for increased IFNγ through the ERK/MAPK pathway. (A) The numbers of infiltrating leukocytes at 12 h post 10 mg/kg Con A challenge were counted (4 mice, each). (B) Hepatic leukocytes were stained with fluorescence-labelled antibodies and percentages of leukocyte populations were analyzed by flow cytometry (4 mice, each). (C) IFNγ-producing cell types in livers at 12 h post 10 mg/kg Con A challenge were examined by flow cytometer (5 mice, each). (D) $CD4^+$ and $D8^+$ T cells isolated from WT- and $Spred2^{-/-}$-spleens were cultured with 10 μg/mL Con A for 6, 12 and 24 h, and IFNγ levels in the culture supernatants were determined (5 mice, each). (E) $CD4^+$ and $CD8^+$ T cells isolated from naive WT and $Spred2^{-/-}$ mice were cultured with plate-bound 10 μg/mL anti-CD3 Ab plus 1 μg/mL anti-CD28 Ab for 48 h. IFNγ levels in the culture supernatants were measured by ELISA (4 samples, each group). (F) $CD4^+$ and $CD8^+$ T cells from naive $Spred2^{-/-}$-spleens were stimulated *in vitro* with 10 μg/mL Con A with 10 μM U0126 or DMSO for 24 h, and IFNγ levels in the supernatants were determined (4 mice for each group). (G) $CD4^+$ and $CD8^+$ T cells from $Spred2^{-/-}$ mice were cultured with 10 μM U0126 or DMSO simultaneously with plate-bound 10 μg/mL anti-CD3 Ab plus 1 μg/mL anti-CD28 Ab for 48 h. IFNγ levels in the supernatants were measured by ELISA (4 samples, each). $^*p < 0.05$., $^{**}p < 0.01$., $^{****}p < 0.0001$.

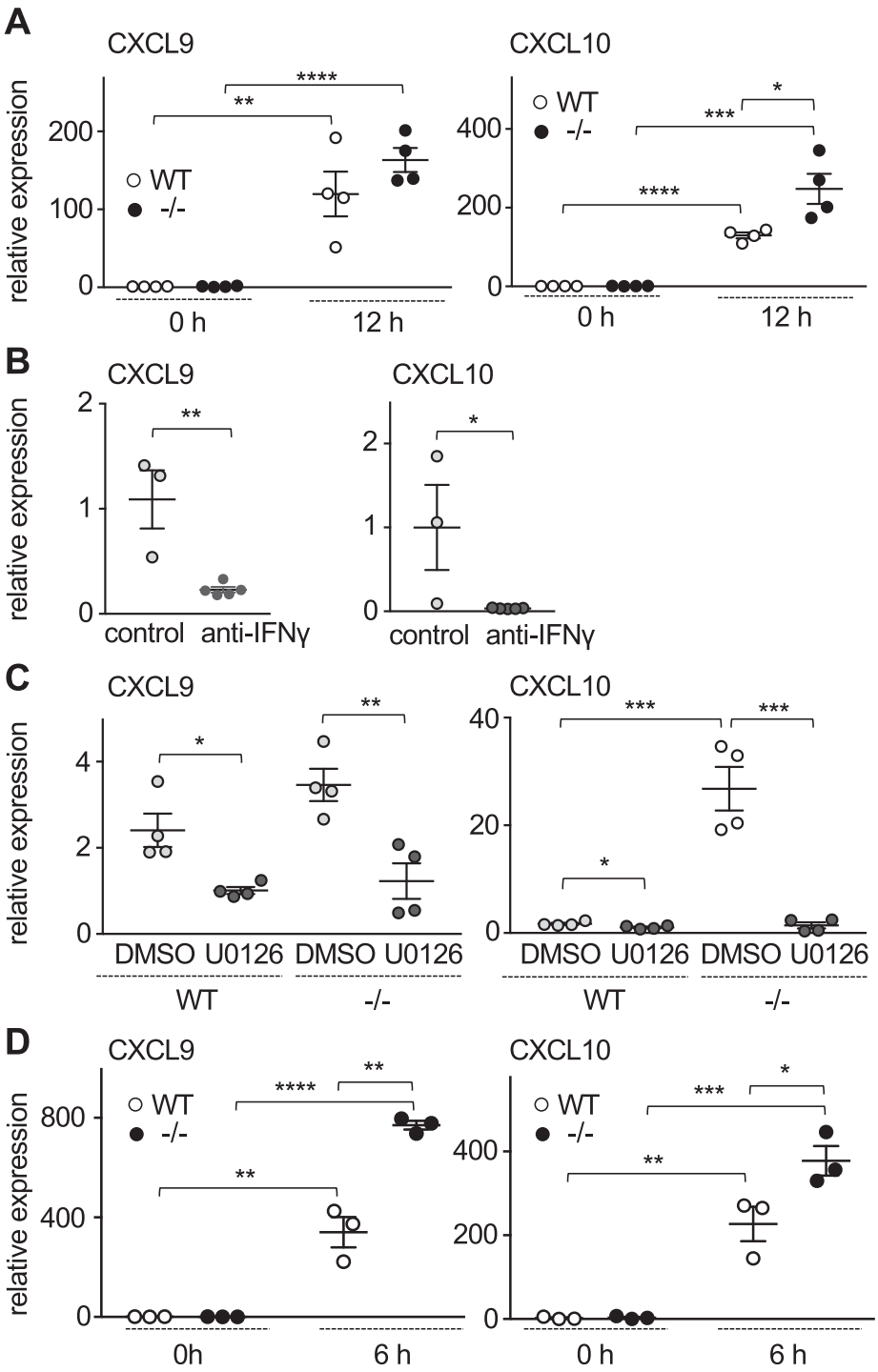

Fig. 6. Enhanced CXCL9 and CXCL10 mRNA expression in Spred2$^{-/-}$-livers. (A) Hepatic mRNA levels of CXCL9 and CXCL10 in WT and Spred2$^{-/-}$ mice at indicated time after 10 mg/kg Con A challenge were quantitated by RT-qPCR (4 mice each). (B) Spred2$^{-/-}$ mice were treated with anti-IFNγ IgG (1 mg/mouse) or control rabbit IgG 12 h prior to 10 mg/kg Con A challenge. Hepatic mRNA levels of CXCL9 and CXCL10 at 12 h post Con A challenge were quantitated by RT-qPCR (3–5 mice, each). (C) WT and Spred2$^{-/-}$ mice were intraperitoneally administered with 10 μmol/kg U0126 or DMSO 3 h prior to 10 mg/kg Con A challenge. mRNA levels of CXCL9 and CXCL10 in livers at 12 h post Con A challenge were analysed by RT-qPCR (4 mice for each group). (D) Hepatocytes isolated from naive WT and Spred2$^{-/-}$ mice were cultured with 40 ng/mL IFNγ for 6 h. mRNA levels of CXCL9 and CXCL10 in livers were quantitated by RT-qPCR (n = 3). *p < 0.05., **p < 0.01., ***p < 0.001., ****p < 0.0001.

Spred2$^{-/-}$-CD8^{+} and WT-CD8^{+} T cells per cell-basis (Fig. 8A), perforin and granzyme B mRNA expressions in Spred2$^{-/-}$-livers were higher than WT controls (Fig. 8B). Of note, number of infiltrating CD8^{+} T cells was larger than WT controls (Fig. 5B). Thus, enhanced CD8^{+} T cell-mediated cytotoxicity by perforin and granzyme B per organ-basis may be involved in more severe hepatocyte damage in mice with Spred2-deficiency.

It is reported that IFNγ can directly cause hepatotoxicity [39]. To examine whether Spred2-deficiency in hepatocytes could affect IFNγ-hepatotoxicity, primary hepatocytes from naive mice were stimulated with IFNγ *in vitro* and levels of LDH, a cell death marker, were measured. As a result, there was no difference between WT- and Spred2$^{-/-}$-hepatocytes (Fig. 8C), indicating that Spred2-deficiency in hepatocytes does not affect the sensitivity to

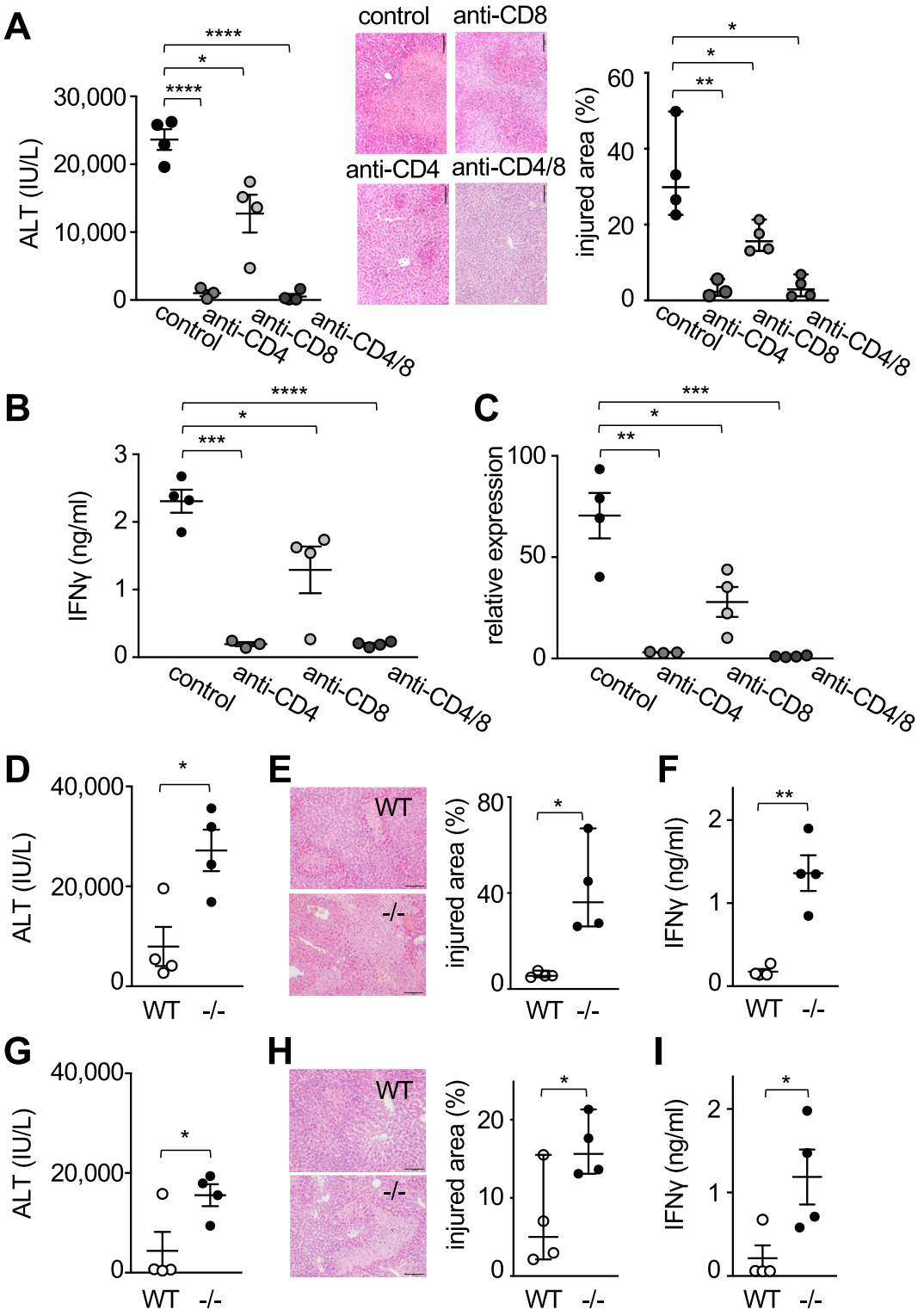

Fig. 7. CD4$^+$ and CD8$^+$ T cells are responsible for Con A-hepatotoxicity. (A-C) Spred2$^{-/-}$ mice were intraperitoneally administered with anti-CD4$^+$ and anti-CD8$^+$ IgG (100 μg/mouse) or control rat IgG 12 h prior to 10 mg/kg Con A challenge. (A) Left, ALT levels in the sera at 12 h post Con A challenge were measured (3–4 mice, each). Right, representative photographs of liver sections are shown (scale bar, 100 μm). %injured area was semi-quantitated using cellSens Standard software. (B) Serum levels of IFNγ at 12 h post Con A challenge were evaluated by ELISA (3–4 mice, each). (C) IFNγ mRNA levels in livers at 12 h post Con A challenge were quantitated by RT-qPCR (3–4 mice, each). (D-I) RAG1$^{-/-}$ mice were intravenously administered through tail vein with CD4$^+$ T cells (2.5 × 10^6 cells/mouse) (D-F, 4 mice each) or CD8$^+$ T cells (5 × 10^6 cells/mouse) (G-I, 4 mice each) isolated from WT or Spred2$^{-/-}$ mice 1 week before 10 mg/kg Con A challenge. (D,G) ALT levels in the sera at 12 h post Con A challenge were measured. (E,H) Left, representative photographs of liver sections are shown (scale bar, 100 μm). Right, %injured area was semi-quantitated using cellSens Standard software. (F,I) IFNγ levels in sera were measured. *p < 0.05., **p < 0.01., ***p < 0.001., ****p < 0.0001.

IFNγ-hepatotoxicity. However, level of IFNγ in Spred2$^{-/-}$ mice was higher than WT mice (Fig. 2A,B). Therefore, it is possible that increased overall IFNγ results in exacerbated liver damage in Spred2$^{-/-}$ mice. Altogether, CD4$^+$ T cells, and to a certain degree CD8$^+$ T cells, appear to contribute to the exacerbated liver damage in Spred2$^{-/-}$ mice by producing higher IFNγ production.

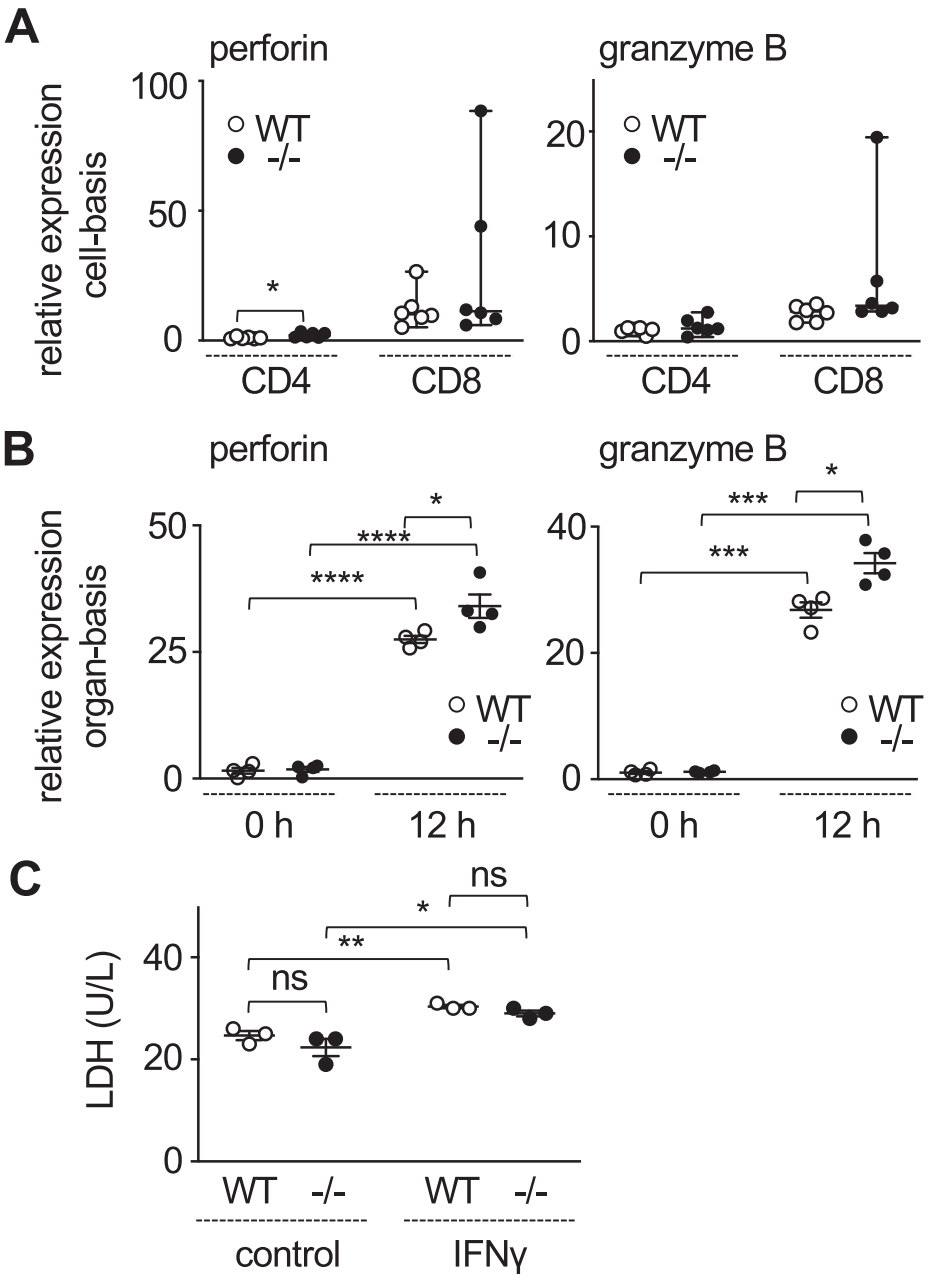

Fig. 8. Hepatocyte damage by $CD4^+/CD8^+$ T cells and IFNγ. (A) Hepatic $CD4^+$ and $CD8^+$ T cells were isolated from WT and $Spred2^{-/-}$ mice at 12 h post 10 mg/kg Con A challenge, and perforin and granzyme B mRNA expressions were quantitated by RT-qPCR (n = 6, each time point). (B) mRNA expressions of perforin and granzyme B in WT and $Spred2^{-/-}$-livers at 12 h post 10 mg/kg Con A challenge were quantitated by RT-qPCR (n = 4, each time point). (C) Hepatocytes isolated from naive WT and $Spred2^{-/-}$ mice were cultured with 40 ng/mL IFNγ for 48 h. Levels of LDH in the culture supernatants were determined (n = 3 each). $^*p < 0.05$., $^{**}p < 0.01$., $^{***}p < 0.001$., $^{****}p < 0.0001$, ns: not significant.

Spred2 overexpression improved Con A-induced liver damage with decreased number of infiltrating $CD4^+$ and $CD8^+$ T cells and IFNγ production

Above results suggested that Con A-hepatoxicity can be improved by overexpression of Spred2. To address this, we employed Spred2 transgenic (Spred2Tg) mice. No difference was found in serum ALT level between naive WT and Spred2Tg mice (29.0 ± 1.7 vs 30.3 ± 2.8 IU/L, respectively, 3 mice each). As expected, Con A-induced liver damage was markedly improved in Spred2Tg mice relative to WT mice with decreased ALT levels (Fig. 9A) and reduced injured area (Fig. 9B) 12 h post Con A challenge. Activation of ERK and Stat1 at 12 h post Con A challenge was decreased in Spred2Tg-livers, as compared to WT-livers (Fig. 9C). The numbers of infiltrating total leukocytes (Fig. 9D) and $CD4^+$ and $CD8^+$ T cells (Fig. 9E) were decreased in Spred2Tg-livers. Levels of serum IFNγ and hepatic IFNγ mRNA expression were lower in Spred2Tg mice than WT mice (Fig. 9F,G). CXCL10 mRNA expression was also decreased in Spred2Tg-livers as compared to WT controls, although CXCL9 levels were not statistically different between the groups (Fig. 9G). To examine whether Spred2 overexpression affects IFNγ production by T cells, splenocytes were isolated from Con A-treated WT and Spred2Tg mice and cultured for 24 h without additional stimulation. As shown in Fig. 9H, splenocytes from Spred2Tg mice released lower level of IFNγ than WT controls. When splenocytes isolated from naive WT and Spred2Tg mice were stimulated with Con A *in vitro*, IFNγ production was significantly reduced in Spred2Tg-splenocytes as compared to WT controls (Fig. 9I) with decreased ERK activation (Fig. 9J). Upon stimulation with Con A *in vitro*, IFNγ production

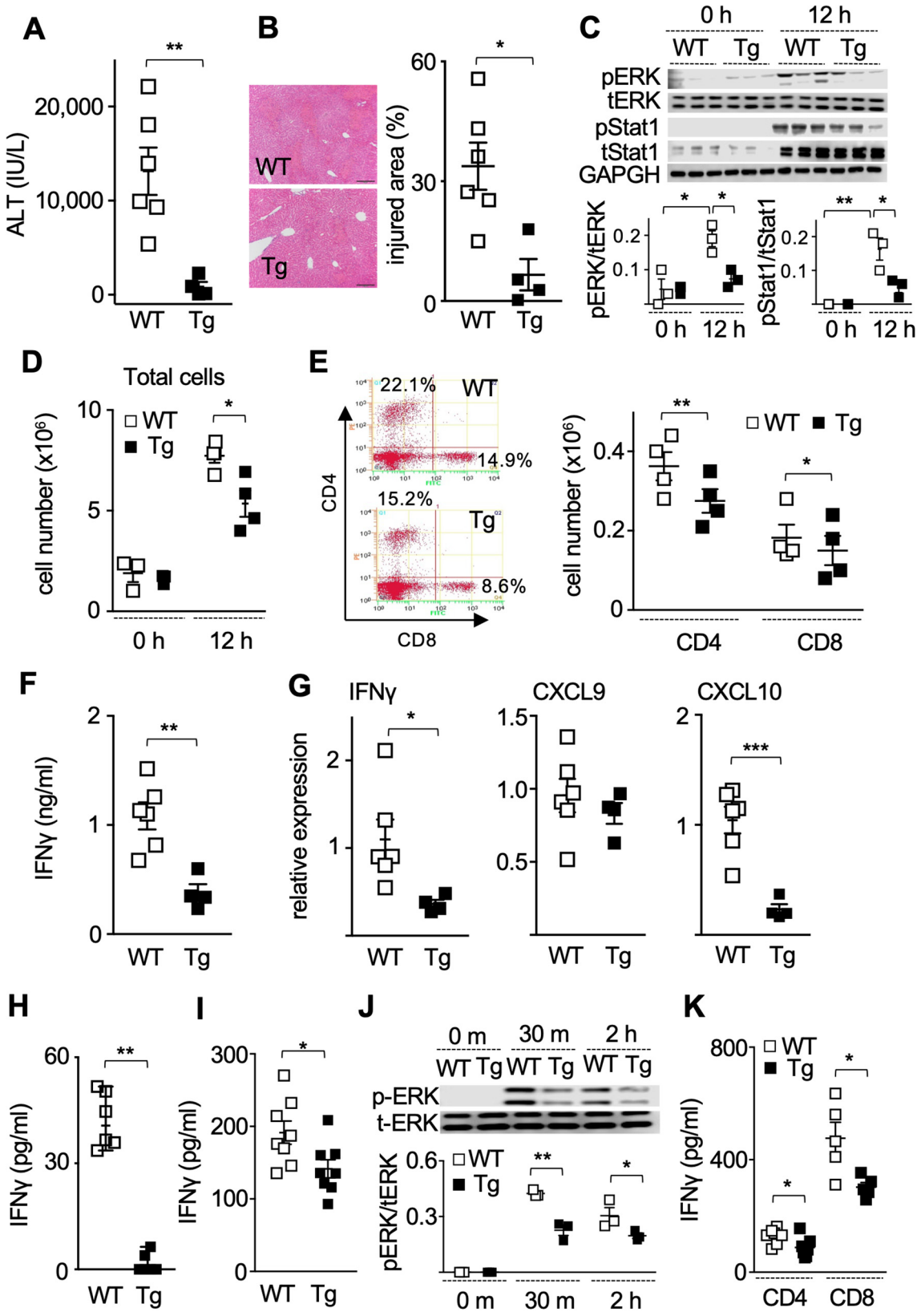
A
ALT (IU/L)
20,000
10,000
0
WT
Tg
B
WT
Tg
injured area (%)
60
30
0
C
0 h
12 h
WT
Tg
pERK
tERK
pStat1
tStat1
GAPGH
pERK/tERK
pStat1/tStat1
0.2
0.1
D
Total cells
cell number (x10⁶)
10
5
0
E
22.1%
14.9%
15.2%
8.6%
CD4
CD8
F
IFNγ (ng/ml)
G
IFNγ
CXCL9
CXCL10
relative expression
H
IFNγ (pg/ml)
60
30
I
300
200
100
J
0 m
30 m
2 h
p-ERK
t-ERK
pERK/tERK
0.6
0.3
K
800
400

Fig. 9. Spred2Tg mice exhibit reduced Con A-induced liver damage. (A) Serum ALT levels in WT and Spred2Tg mice were measured post 12 h 10 mg/kg Con A challenge (WT; 6 mice, Spred2Tg; 4 mice). (B) Left; liver sections from WT and Spred2Tg mice at 12 h post 10 mg/kg Con A challenge (scale bar, 100 μm). Right; %injured area was estimated using the cellSens Standard software (WT; 6 mice, Spred2Tg; 4 mice). (C) Liver extracts at 12 h post 10 mg/kg Con A challenge were immunoblotted with indicated primary antibodies (3 mice each). Band densities were digitised and semi-quantitated. (D) The numbers of infiltrating leukocytes at 12 h post 10 mg/kg Con A challenge were counted (4 mice, each). (E) Hepatic leukocytes were stained with fluorescence-labelled antibodies and percentages of leukocyte populations were analyzed by flow cytometry (4 mice, each). (F) Serum IFNγ level was measured by ELISA at 12 h post 10 mg/kg Con A challenge (WT; 6 mice, Spred2Tg; 4 mice). (G) IFNγ, CXCL9 and CXCL10 mRNA expressions in WT and Spred2Tg-livers at 12 h post 10 mg/kg Con A challenge were quantitated by RT-qPCR (WT; 6 mice, Spred2Tg; 4 mice). (H) Splenocytes harvested from WT and Spred2Tg mice at 12 h post 10 mg/kg Con A challenge were cultured for 24 h without additional stimulation (n = 6). IFNγ levels in the culture supernatants were measured. (I) Splenocytes isolated from naive WT and Spred2Tg mice were cultured with 10 μg/mL Con A for 24 h and IFNγ levels in the supernatants were determined. (J) Splenocytes isolated from naive WT and Spred2Tg mice were cultured with 10 μg/mL Con A for 30 min and 2 h. The level of each protein in cells was evaluated by Western blotting using the indicated primary antibodies (3 each). Band densities were digitised and semi-quantitated. (K) $CD4^+$ and $CD8^+$ T cells from untreated WT- and Spred2Tg-spleens were cultured with 10 μg/mL Con A for 24 h, and IFNγ levels in the culture supernatants were determined (n = 5, each). $^*p < 0.05$., $^{**}p < 0.01$., $^{***}p < 0.001$.

from naive Spred2Tg-$CD4^+$ and -$CD8^+$ T cells were lower than WT controls (Fig. 9K). Thus, Spred2 overexpression improves Con A-hepatotoxicity by reducing IFNγ production from $CD4^+$ and $CD8^+$ T cells, further confirming the significant impact of Spred2 on T cell IFNγ production and T cell-mediated liver damage.

Discussion

In the present study, we demonstrated that Spred2 that negatively regulates ERK-MAPK is protective during Con A-induced liver damage via decreased IFNγ production from $CD4^+$ and $CD8^+$ T cells. $CD4^+$ T cells are the main sources of IFNγ [40] and are harmful immune cell subsets in Con A-hepatotoxicity [8]. $CD8^+$ T cells were accumulated in livers after Con A challenge in mice [41] and in livers from patients with AIH [42]. IFNγ production was detected in $CD8^+$ T cells after Con A-challenge [9]. Here, we showed by the depletion and transplantation of $CD4^+$ and $CD8^+$ T cells that Spred2-deficiency in $CD4^+$ and $CD8^+$ T cells are responsible for the augmented IFNγ production, leading to the exacerbated Con A-hepatotoxicity.

T cell antigen receptor (TCR) ligation leads to the activation of ERK and subsequent IFNγ production [30]. In addition to Con A, direct activation of TCR on $CD4^+$ and $CD8^+$ T cells with anti-CD3/CD28 also resulted in increased IFNγ production by $Spred2^{-/-}$-T cells *in vitro*. Activation of ERK and Stat1 was enhanced in $Spred2^{-/-}$ splenocytes, and the Stat1 activation was inhibited by a MAPK/ERK inhibitor U0126. Activation of Stat1 as well as ERK was decreased in livers of Con A-treated Spred2Tg mice. Further, IFNγ production by splenocytes and $CD4^+$/$CD8^+$ T cells from Spred2Tg mice was decreased as compared to WT T cells. These results suggest that endogenous Spred2 can inhibit IFNγ production by $CD4^+$ and $CD8^+$ T cells by modulating the ERK/MAPK pathway that also influences the Stat1 pathway. We examined the expression of Spred2 mRNA in WT-$CD4^+$ and $CD8^+$ T cells after stimulation with Con A *in vitro*. Spred2 mRNA level increased at 6 h but dramatically decreased by 12 h and remained low at 24 h, which may allow more efficient IFNγ production by T cells (Fig. S2). It will be interesting to examine the mechanism(s) of Spred2 expression in T cells and the impact of Spred2 in other functions of T cells.

Stat1 and Stat3 were previously shown to regulate each other in Con A-induced liver injury. Disruption of Stat1 attenuated Con A-liver injury, but enhanced Stat3 activation and Stat3-controlled antiapoptotic signals. Downregulation of Stat3 activation was associated with enhanced Stat1 activation and Stat1-induced exacerbation of liver injury, suggesting opposing roles of Stat1 and Stat3 in T cell-mediated hepatitis thorough the induction of suppressor of cytokine signaling (SOCS) [29]. In our study, both Stat1 and Stat3 were activated in WT-livers after Con A challenge. Since Stat1 activation was enhanced in $Spred2^{-/-}$-livers by increased IFNγ response, Stat3 activation could be altered in $Spred2^{-/-}$-livers. However, no difference was found in Stst3 activation in $Spred2^{-/-}$-livers as compared to WT-controls. In response to IFNγ, not only Stat1 but Stat3 can be weakly activated [43], in which Stat1-independent induction of SOCS3 by IFNγ may play a role [44]. Thus, activation of Stat1 and Stat3 in response to IFNγ may vary under different conditions. Further research is needed to address this possibility.

Our results suggest that Spred2-deficiency in T cells plays a central role in the enhanced Con A-hepatotoxicity. However, other cell types, including macrophages, neutrophils and hepatocytes, can also be stimulated by IFNγ *in vivo*. Enhanced ERK and Stat1 activation in the liver could be due to the activation of these cells. We recently generated myeloid cell-specific $Spred2^{-/-}$ mice, by crossing Spred2-floxed mice with LysMCre mice [45]. LysMcre mice are useful to delete genes in myeloid cells, including macrophages, neutrophils [46] and Kupffer cells [47]. No differences were observed in serum ALT levels, hepatic number of $CD4^+$ and $CD8^+$ T cells, or hepatic IFNγ/TNFα/CXCL9/CXCL10 mRNA expression levels between $LysMCre^+$:$Spred2^{fl/fl}$ and $Spred2^{fl/fl}$ mice (Fig. S5). Macrophages and Kupffer cells are known as the cellular sources of CXCL9 and CXC10 in Con A-hepatitis [35]. Although we previously showed that $Spred2^{-/-}$-Kupffer cells expressed higher levels of CXCL9 and CXCL10 after stimulation with IFNγ [18], CXCL9 and CXCL10 production appears to be more dependent on hepatocytes than Kupffer cells in Con A-hepatotoxicity. Considering the results obtained by myeloid cell-specific $Spred2^{-/-}$ mice and $Spred2^{-/-}$-hepatocytes, deficiency of Spred2 in myeloid cells or hepatocytes does not appear involved in the enhanced hepatotoxicity.

Chemokines are important in the development of inflammation by attracting diverse inflammatory cells into injured tissues. In this study, CXCL9 and CXCL10 mRNA expressions in $Spred2^{-/-}$-livers were higher than WT controls, which were significantly inhibited by neutralization of IFNγ. A MAPK/ERK inhibitor U0126 decreased CXCL9 and CXCL10 mRNA expression in $Spred2^{-/-}$-livers after Con A challenge. Thus, enhanced IFNγ production in $Spred2^{-/-}$ mice results in enhanced production of CXCL9 and CXCL10 through ERK/MAPK. Hepatocytes are known to produce CXCL9 and CXCL10 upon IFNγ stimulation [35,36]. We showed in this study that $Spred2^{-/-}$-hepatocytes expressed augmented levels of CXCL9 and CXCL10 after stimulation with IFNγ. Thus, it appears that Spred2-deficiency in $CD4^+$ and $CD8^+$ T cells leads to higher IFNγ level in response to Con A, and this increased level of IFNγ stimulates hepatocytes to produce CXCL9 and CXCL10. CXCL9 and CXCL10 attract $CD4^+$ and $CD8^+$ T cells [48,49]. Elevated hepatic CXCL9 and CXCL10 in $Spred2^{-/-}$ mice recruit additional $CD4^+$ and $CD8^+$ T cells in livers, which then lead to additional IFNγ secretion that induces elevated CXCL9 and CXCL10 production in livers. Based on this positive feedback loop, Con A-hepatotoxicity appears to be exacerbated in $Spred2^{-/-}$ mice.

Conclusion

Our results demonstrated that Spred2-deficiency results in increased IFNγ production by $CD4^+$ and $CD8^+$ T cells and more severe liver damage due to up-regulated ERK in response to Con A injection. Conversely, Spred2 overexpression decreases IFNγ production by $CD4^+$ and $CD8^+$ T cells and improves Con A-hepatotoxicity. Furthermore, Spred2 overexpressing-splenocytes, -$CD4^+$ and -$CD8^+$ T cells produced lower levels of IFNγ than WT controls upon stimulation with ConA *in vitro*. These results indicate that Spred2 is a novel regulator of T cell IFNγ production and Spred2-mediated inhibition of the ERK-MAPK pathway may be a new remedy for T cell-dependent liver damage.

Compliance with Ethics Requirements

All Institutional and National Guidelines for the care and use of animals (fisheries) were followed.

Declaration of Competing Interest

The authors declare that they have no known competing financial interests or personal relationships that could have appeared to influence the work reported in this paper.

Acknowledgements

We thank Dr. Akihiko Yoshimura and Dr. Eiichi Nakayama for providing $Spred2^{-/-}$ mice and anti-CD4/CD8 antibodies, respectively. We thank Mr. Hiroyuki Watanabe for the technical support. This work was supported by JSPS KAKENHI, 25293095 and 16K15258.

Appendix A. Supplementary material

Supplementary data to this article can be found online at https://doi.org/10.1016/j.jare.2021.03.014.

References

[1] Kita H, Mackay IR, Van De Water J, Gershwin ME. The lymphoid liver: considerations on pathways to autoimmune injury. Gastroenterology 2001;120(6):1485–501.
[2] Rehermann B, Chisari FV. Cell mediated immune response to the hepatitis C virus. Curr Top Microbiol Immunol 2000;242:299–325.
[3] Chang KM, Thimme R, Melpolder JJ, Oldach D, Pemberton J, Moorhead-Loudis J, et al. Differential CD4(+) and CD8(+) T-cell responsiveness in hepatitis C virus infection. Hepatology 2001;33(1):267–76.
[4] Longhi MS, Ma Y, Mieli-Vergani G, Vergani D. Aetiopathogenesis of autoimmune hepatitis. J Autoimmun 2010;34(1):7–14.
[5] Leifeld L, Cheng S, Ramakers J, Dumoulin FL, Trautwein C, Sauerbruch T, et al. Imbalanced intrahepatic expression of interleukin 12, interferon gamma, and interleukin 10 in fulminant hepatitis B. Hepatology 2002;36(4 Pt 1):1001–8.
[6] Sobue S, Nomura T, Ishikawa T, Ito S, Saso K, Ohara H, et al. Th1/Th2 cytokine profiles and their relationship to clinical features in patients with chronic hepatitis C virus infection. J Gastroenterol 2001;36(8):544–51.
[7] Vergani D, Longhi MS, Bogdanos DP, Ma Y, Mieli-Vergani G. Autoimmune hepatitis. Semin Immunopathol 2009;31(3):421–35.
[8] Tiegs G, Hentschel J, Wendel A. A T cell-dependent experimental liver injury in mice inducible by concanavalin A. J Clin Invest 1992;90(1):196–203.
[9] Miyagi T, Takehara T, Tatsumi T, Suzuki T, Jinushi M, Kanazawa Y, et al. Concanavalin a injection activates intrahepatic innate immune cells to provoke an antitumor effect in murine liver. Hepatology 2004;40(5):1190–6.
[10] Küsters S, Gantner F, Künstle G, Tiegs G. Interferon gamma plays a critical role in T cell-dependent liver injury in mice initiated by concanavalin A. Gastroenterology 1996;111(2):462–71.
[11] Tagawa Y, Sekikawa K, Iwakura Y. Suppression of concanavalin A-induced hepatitis in IFN-gamma(-/-) mice, but not in TNF-alpha(-/-) mice: role for IFN-gamma in activating apoptosis of hepatocytes. J Immunol 1997;159(3):1418–28.
[12] Arthur JS, Ley SC. Mitogen-activated protein kinases in innate immunity. Nat Rev Immunol 2013;13(9):679–92.
[13] Horiuchi M, Itoh A, Pleasure D, Itoh T. MEK-ERK signaling is involved in interferon-gamma-induced death of oligodendroglial progenitor cells. J Biol Chem 2006;281(29):20095–106.
[14] Tu CT, Li J, Wang FP, Li L, Wang JY, Jiang W. Glycyrrhizin regulates CD4+T cell response during liver fibrogenesis via JNK, ERK and PI3K/AKT pathway. Int Immunopharmacol 2012;14(4):410–21.
[15] Wakioka T, Sasaki A, Kato R, Shouda T, Matsumoto A, Miyoshi K, et al. Spred is a Sprouty-related suppressor of Ras signalling. Nature 2001;412(6847):647–51.
[16] Itakura J, Sato M, Ito T, Mino M, Fushimi S, Takahashi S, et al. Spred2-deficiecy Protects Mice from Polymicrobial Septic Peritonitis by Enhancing Inflammation and Bacterial Clearance. Sci Rep 2017;7(1):12833.
[17] Ohkura T, Yoshimura T, Fujisawa M, Ohara T, Marutani R, Usami K, et al. Spred2 Regulates High Fat Diet-Induced Adipose Tissue Inflammation, and Metabolic Abnormalities in Mice. Front Immunol 2019;10:17.
[18] Wakabayashi H, Ito T, Fushimi S, Nakashima Y, Itakura J, Qiuying L, et al. Spred-2 deficiency exacerbates acetaminophen-induced hepatotoxicity in mice. Clin Immunol 2012;144(3):272–82.
[19] Xu Y, Ito T, Fushimi S, Takahashi S, Itakura J, Kimura R, et al. Spred-2 deficiency exacerbates lipopolysaccharide-induced acute lung inflammation in mice. PLoS ONE 2014;9:e108914.
[20] Yang X, Fujisawa M, Yoshimura T, Ohara T, Sato M, Mino M, et al. Spred2 Deficiency Exacerbates D-Galactosamine/Lipopolysaccharide -induced Acute Liver Injury in Mice via Increased Production of TNFα. Sci Rep 2018;8(1):188.
[21] L. Yuan, N. Kaplowitz. Mechanisms of drug-induced liver injury. Clin Liver Dis, 17(4) (2013), 507-18, vii.
[22] Leist M, Gantner F, Bohlinger I, Tiegs G, Germann PG, Wendel A. Tumor necrosis factor-induced hepatocyte apoptosis precedes liver failure in experimental murine shock models. Am J Pathol 1995;146(5):1220–34.
[23] Nobuhisa I, Kato R, Inoue H, Takizawa M, Okita K, Yoshimura A, et al. Spred-2 suppresses aorta-gonad-mesonephros hematopoiesis by inhibiting MAP kinase activation. J Exp Med 2004;199(5):737–42.
[24] Niwa H, Yamamura K, Miyazaki J. Efficient selection for high-expression transfectants with a novel eukaryotic vector. Gene 1991;108(2):193–9.
[25] Mieno M, Suto R, Obata Y, Udono H, Takahashi T, Shiku H, et al. CD4-CD8- T cell receptor alpha beta T cells: generation of an in vitro major histocompatibility complex class I specific cytotoxic T lymphocyte response and allogeneic tumor rejection. J Exp Med 1991;174(1):193–201.
[26] Seglen PO. Preparation of isolated rat liver cells. Methods Cell Biol 1976;13:29–83.
[27] Fushimi S, Ogino T, Hara J, Takahata T, Wakabayashi H, Watanabe H, et al. Forced expression of suppressor of cytokine signaling 3 in T cells protects the development of concanavalin A-induced hepatitis in mice. Clin Immunol 2009;133(3):437–46.
[28] Kremer M, Hines IN, Milton RJ, Wheeler MD. Favored T helper 1 response in a mouse model of hepatosteatosis is associated with enhanced T cell-mediated hepatitis. Hepatology 2006;44(1):216–27.
[29] Hong F, Jaruga B, Kim WH, Radaeva S, El-Assal ON, Tian Z, et al. Opposing roles of STAT1 and STAT3 in T cell-mediated hepatitis: regulation by SOCS. J Clin Invest 2002;110(10):1503–13.
[30] Kortum RL, Rouquette-Jazdanian AK, Samelson LE. Ras and extracellular signal-regulated kinase signaling in thymocytes and T cells. Trends Immunol 2013;34(6):259–68.
[31] Zheng C, Yin S, Yang Y, Yu Y, Xie X. CD24 aggravates acute liver injury in autoimmune hepatitis by promoting IFN-γ production by $CD4^+$ T cells. Cell Mol Immunol 2018;15(3):260–71.
[32] Zhang S, Liang R, Luo W, Liu C, Wu X, Gao Y, et al. High susceptibility to liver injury in IL-27 p28 conditional knockout mice involves intrinsic interferon-γ dysregulation of CD4+ T cells. Hepatology 2013;57(4):1620–31.
[33] Trickett A, Kwan YL. T cell stimulation and expansion using anti-CD3/CD28 beads. J Immunol Methods 2003;275(1–2):251–5.
[34] Saiman Y, Friedman SL. The role of chemokines in acute liver injury. Front Physiol 2012;3:213.
[35] Jaruga B, Hong F, Kim WH, Gao B. IFN-gamma/STAT1 acts as a proinflammatory signal in T cell-mediated hepatitis via induction of multiple chemokines and adhesion molecules: a critical role of IRF-1. Am J Physiol Gastrointest Liver Physiol 2004;287(5):G1044–52.
[36] Ren X, Kennedy A, Colletti LM. CXC chemokine expression after stimulation with interferon-gamma in primary rat hepatocytes in culture. Shock 2002;17(6):513–20.
[37] Kaneko Y, Harada M, Kawano T, Yamashita M, Shibata Y, Gejyo F, et al. Augmentation of Valpha14 NKT cell-mediated cytotoxicity by interleukin 4 in an autocrine mechanism resulting in the development of concanavalin A-induced hepatitis. J Exp Med 2000;191(1):105–14.
[38] Pham BN, Martinot-Peignoux M, Valla D, Dubois S, Degott C, Mosnier JF. Differential expression of perforin and granzyme B in the liver of patients with chronic hepatitis C. Hum Pathol 2003;34(8):770–7.
[39] Morita M, Watanabe Y, Akaike T. Protective effect of hepatocyte growth factor on interferon-gamma-induced cytotoxicity in mouse hepatocytes. Hepatology 1995;21(6):1585–93.
[40] Watanabe Y, Morita M, Akaike T. Concanavalin A induces perforin-mediated but not Fas-mediated hepatic injury. Hepatology 1996;24(3):702–10.
[41] Yamashita J, Iwamura C, Sasaki T, Mitsumori K, Ohshima K, Hada K, et al. Apolipoprotein A-II suppressed concanavalin A-induced hepatitis via the inhibition of CD4 T cell function. J Immunol 2011;186(6):3410–20.

[42] Taubert R, Hardtke-Wolenski M, Noyan F, Wilms A, Baumann AK, Schlue J, et al. Intrahepatic regulatory T cells in autoimmune hepatitis are associated with treatment response and depleted with current therapies. J Hepatol 2014;61(5):1106–14.
[43] Qing Y, Stark GR. Alternative activation of STAT1 and STAT3 in response to interferon-gamma. J Biol Chem 2004;279(40):41679–85.
[44] Ramana CV, Kumar A, Enelow R. Stat1-independent induction of SOCS-3 by interferon-gamma is mediated by sustained activation of Stat3 in mouse embryonic fibroblasts. Biochem Biophys Res Commun 2005;327(3):727–33.
[45] Kawara A, Mizuta R, Fujisawa M, Ito T, Li C, Nakamura K, et al. Spred2-deficiency enhances the proliferation of lung epithelial cells and alleviates pulmonary fibrosis induced by bleomycin. Sci Rep 2020;10(1):16490.
[46] Clausen BE, Burkhardt C, Reith W, Renkawitz R, Förster I. Conditional gene targeting in macrophages and granulocytes using LysMcre mice. Transgenic Res 1999;8(4):265–77.
[47] Zhang Z, Zhang F, An P, Guo X, Shen Y, Tao Y, et al. Ferroportin1 deficiency in mouse macrophages impairs iron homeostasis and inflammatory responses. Blood 2011;118(7):1912–22.
[48] Dufour JH, Dziejman M, Liu MT, Leung JH, Lane TE, Luster AD. IFN-gamma-inducible protein 10 (IP-10; CXCL10)-deficient mice reveal a role for IP-10 in effector T cell generation and trafficking. J Immunol 2002;168(7):3195–204.
[49] Ochiai E, Sa Q, Brogli M, Kudo T, Wang X, Dubey JP, et al. CXCL9 is important for recruiting immune T cells into the brain and inducing an accumulation of the T cells to the areas of tachyzoite proliferation to prevent reactivation of chronic cerebral infection with Toxoplasma gondii. Am J Pathol 2015;185(2):314–24.